



Li-doped *N*-methoxyethyl-*N*-methylpyrrolidinium fluorosulfonyl-(trifluoromethanesulfonyl)imide as electrolyte for reliable lithium ion batteries

Arianna Moretti^a, Sangsik Jeong^a, Guinevere A. Giffin^a, Sebastian Jeremias^a, Stefano Passerini^{a, b, c, *}

^a Institute of Physical Chemistry and MEET Battery Research Center, University of Muenster, Corrensstrasse 28, 48149 Muenster, Germany

^b Helmholtz Institute Ulm (HIU), Electrochemistry Ic, Albert Einstein Allee 11, 89081 Ulm, Germany

^c Karlsruhe Institute of Technology (KIT), P.O. Box 3640, 76021 Karlsruhe, Germany

HIGHLIGHTS

- Enhanced performance of ILs based on fluorosulfonyl-(trifluoromethanesulfonyl) imide (FTFSI).
- PYR₁₂₀₁FTFSI-LiFTFSI offers excellent electrochemical performance at room temperature.
- Remarkable performance of LTO/PYR₁₂₀₁FTFSI-LiFTFSI/LFP cells at room temperature.
- High stability of LTO/PYR₁₂₀₁FTFSI-LiFTFSI/LFP cells at elevated temperature.

ARTICLE INFO

Article history:

Received 1 February 2014

Received in revised form

20 June 2014

Accepted 30 June 2014

Available online 11 July 2014

Keywords:

Lithium ion battery

Ionic liquids

N-Methoxyethyl-*N*-methylpyrrolidinium fluorosulfonyl-(trifluoromethanesulfonyl) imide

LiFePO₄

Li₄Ti₅O₁₂

Electrochemical performance

ABSTRACT

The electrochemical performance of a new electrolyte based on *N*-methoxyethyl-*N*-methylpyrrolidinium fluorosulfonyl-(trifluoromethanesulfonyl)imide (PYR₁₂₀₁FTFSI) doped with LiFTFSI salt has been investigated. The electrolyte showed no evidence of crystalline phases even at low temperatures and possesses high ionic conductivity ($3.7 \times 10^{-3} \text{ S cm}^{-1}$ at 20 °C) that makes it suitable for lithium battery applications. The new electrolyte has been tested in combination with aqueous processed, electrode materials such as Li₄Ti₅O₁₂ and LiFePO₄, showing good electrochemical performance even at room temperature. Lab-scale, lithium-ion cells comprising Li₄Ti₅O₁₂/PYR₁₂₀₁FTFSI-LiFTFSI/LiFePO₄ were also assembled and tested. The cells exhibit stable cycling behavior at room temperature with an energy density of 130 Wh kg⁻¹. Moreover, the cell was cycled at 1C up to 80 °C displays a capacity loss of about 30% but retaining high coulombic efficiency. These results demonstrate the feasibility of PYR₁₂₀₁FTFSI-based ionic liquids as electrolytes for safer and greener lithium ion batteries with extended operative temperature range.

© 2014 Elsevier B.V. All rights reserved.

1. Introduction

Lithium ion batteries (LIBs) are currently dominating the portable electronic market and are considered the most promising technology for next generation hybrid and electric vehicles. However, wide spread implementation of LIBs in the automotive market depends on costs reduction and safety improvements [1].

The main safety issues arise from the utilization of organic solvents as electrolytes media, generally alkylcarbonates as EC, DMC and DEC, that are highly flammable, thermally unstable, volatile and toxic [2,3]. Alternative safer electrolytes, which at the same time fulfill the requirements of high ionic conductivity and large electrochemical stability, are thus under intense investigation. Ionic liquids (ILs) are room temperature molten salts that possess ideal characteristics for such a kind of application [4,5]. Indeed, they are non-flammable and non-volatile, possess excellent thermal and electrochemical stabilities and allow lithium ion conduction [6]. Furthermore, their chemical and physical properties can be tuned by selecting the appropriate cation/anion combination. Recently, electrolytes based on the coupling of pyrrolidinium

* Corresponding author. Institute of Physical Chemistry and MEET Battery Research Center, University of Muenster, Corrensstrasse 28, 48149 Muenster, Germany.

E-mail addresses: stefano.passerini@kit.edu, stefano.passerini@uni-muenster.de (S. Passerini).

cations with imide anions, mainly bis(trifluoromethanesulfonyl) imide (TFSI) and bis(fluorosulfonyl)imide (FSI), have gained increased attention because they exhibit, among other ILs systems, very large electrochemical stability windows [7,8]. However, the utilization of these ILs in electrochemical devices is hindered by their tendency to crystallize that limits the working temperature range [9,10].

To overcome this drawback, and exploiting the possibility of tailoring ILs properties by chemical modifications, our group recently synthesized and characterized a new ionic liquid, *N*-methoxyethyl-*N*-methylpyrrolidinium fluorosulfonyl-(trifluoromethanesulfonyl)imide (PYR₁₂₀₁FTFSI) based on the introduction of an ether functionality in the ammonium cation side chain and the asymmetric imide anion with the lowest MW [11–13]. The concept simultaneously takes advantage of the introduction of a flexible methoxyethyl chain in the cation, to increase fluidity and conductivity, and the use of an asymmetric anion to lower, or even prevent the crystallization [14,15]. Indeed, the obtained IL showed the absence of any detectable crystallization down to $-150\text{ }^{\circ}\text{C}$ and conductivity values higher than 10^{-4} S cm^{-1} even at $-40\text{ }^{\circ}\text{C}$. As shown in an earlier work, ionic liquids containing the FTFSI anion possess properties intermediate of those of FSI and TFSI-based ionic liquids [12].

In this paper we extend the characterization of PYR₁₂₀₁FTFSI to the electrochemical properties showing, for the first time, the application of PYR₁₂₀₁FTFSI–LiTFSI electrolyte in a lithium-ion battery.

We focused on Li₄Ti₅O₁₂ and LiFePO₄ electrodes as they are considered the cheapest, safer and greener materials. To stress furthermore that environmental friendly, low-cost batteries are feasible, we used water-processed electrode materials avoiding the toxic and expensive fluorinated binder (PVDF) and organic solvent (NMP) [16–19]. Moreover the behavior of this lithium-ion cell at high temperature is compared to that of a cell made with a conventional carbonate-based electrolyte to show that the use of ILs, in combination with LTO and LFP permits the extension of the temperature range of the battery.

2. Experimental

PYR₁₂₀₁FTFSI was synthesized as reported in Ref. [20]. The LiTFSI salt (Provisco CS Ltd. Czech Republic) was dried under vacuum at room temperature for 24 h with a turbomolecular pump (10^{-7} bar). PYR₁₂₀₁FTFSI and LiTFSI were then mixed in the molar ratio of 9:1. The obtained electrolyte was dried again at room temperature for 24 h with a vacuum oil pump (10^{-3} bar) and additionally 24 h with a turbomolecular pump. Unless otherwise stated, all sample preparation was carried out in a dry room (dew point $< -50\text{ }^{\circ}\text{C}$).

Differential Scanning Calorimetry measurements (DSC) were made on a TA Instruments Q2000 differential scanning calorimeter. The samples were hermetically sealed in an aluminum pans. The thermal treatment included cycling ($5\text{ }^{\circ}\text{C min}^{-1}$) at sub-ambient temperatures with isothermal steps at the high end of the temperature range to promote crystallization prior to the first full heating cycle (-150 to $80\text{ }^{\circ}\text{C}$, $5\text{ }^{\circ}\text{C min}^{-1}$).

The temperature dependence of the electrolyte conductivity was measured from $-40\text{ }^{\circ}\text{C}$ up to $70\text{ }^{\circ}\text{C}$ in $2\text{ }^{\circ}\text{C}$ steps. The sample was loaded in a sealed conductivity cell containing two platinum electrodes (MaterialMates, Italy). The cell constant was calibrated using a 0.01 M KCl aqueous solution. The cell was then immersed in a thermostatic bath (Julabo FP50) and cooled down to $-40\text{ }^{\circ}\text{C}$ for 18 h before starting to increase the temperature. The electrolyte was left to equilibrate for 30–40 min at each temperature before acquiring the impedance spectra (VMP3, BioLogic) in the

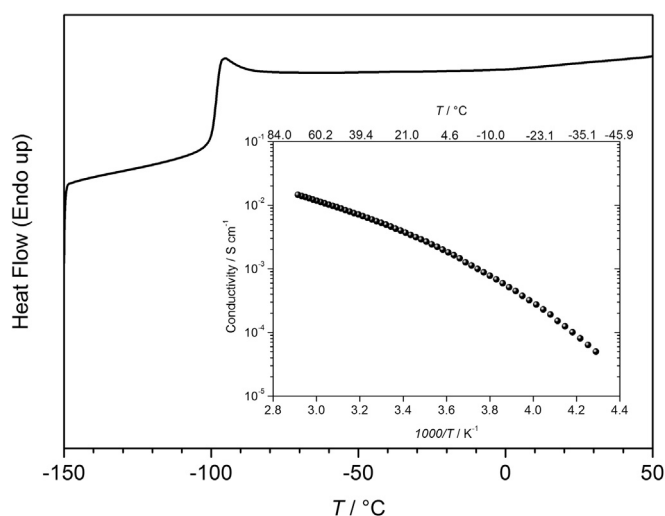


Fig. 1. Phase behavior of PYR₁₂₀₁FTFSI–LiTFSI (9:1) electrolyte. DSC heating trace at $5\text{ }^{\circ}\text{C min}^{-1}$ and, in the inset, temperature dependence of ionic conductivity.

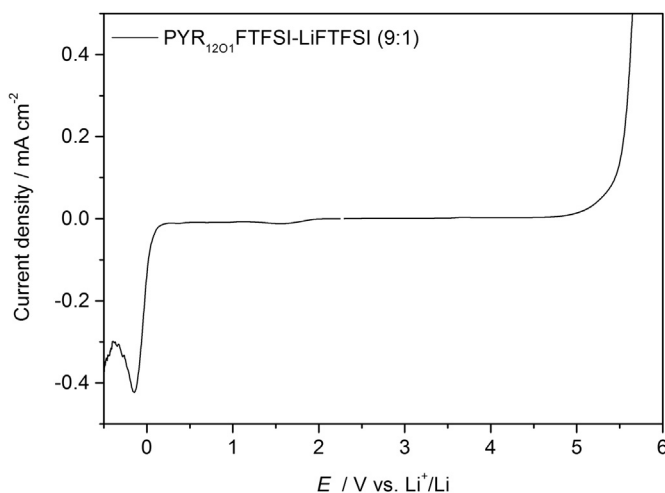


Fig. 2. Linear sweep voltammograms of PYR₁₂₀₁FTFSI–LiTFSI (9:1) electrolyte measured at room temperature with a scan rate of 1 mV s^{-1} (Pt working electrode).

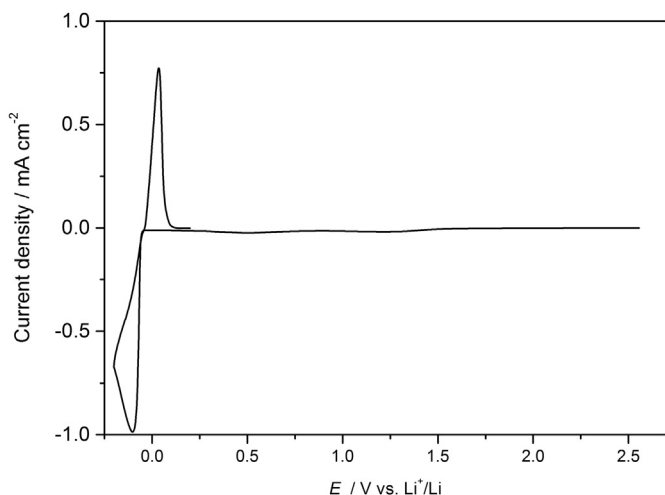


Fig. 3. Cyclic voltammetry for the lithium stripping-plating process in PYR₁₂₀₁FTFSI–LiTFSI (9:1) electrolyte at room temperature. Scan rate 0.1 mV s^{-1} . Working electrode: polished nickel foil.

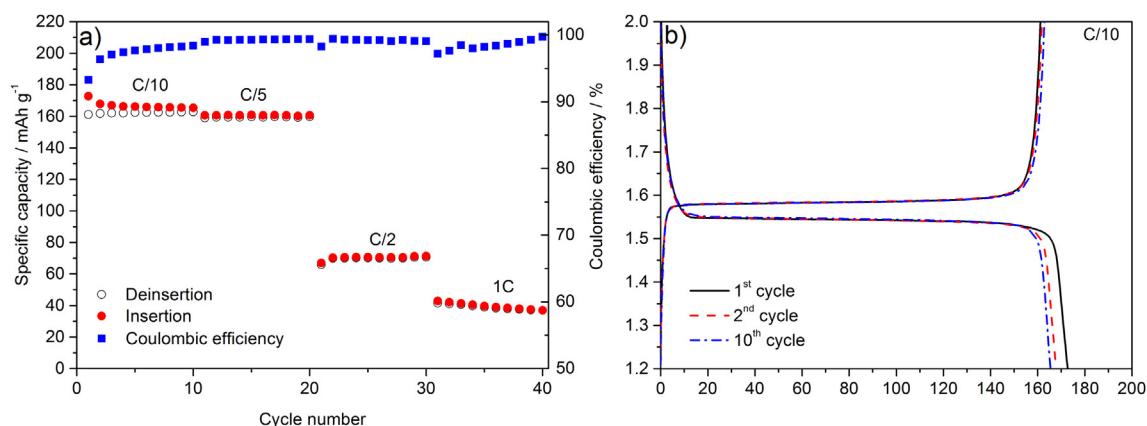


Fig. 4. a) Specific charge, discharge and coulombic efficiency obtained at different C-rates for $\text{Li}_4\text{Ti}_5\text{O}_{12}$ electrodes in combination with $\text{PYR}_{1201}\text{FTFSI-LiFTFSI}$ (9:1) electrolyte. b) Voltage profiles for some selected cycles at C/10 rate.

1 MHz–1 Hz frequency range (10 mV signal amplitude). The spectra were analyzed using the EC-Lab software. The resulting ohmic resistances were converted to specific conductivity using the cell constant previously determined.

The electrochemical tests were conducted at room temperature (20 °C) using three-electrode Swagelok cells assembled in a glovebox (MBraun) under argon atmosphere (water and oxygen contents below 1 ppm).

The electrochemical stability window (ESW) of the electrolyte was evaluated by linear sweep voltammetry (LSV) using modified Swagelok cells. Li metal foil (ROCKWOOD Lithium, battery grade) was used for the counter and reference electrodes while a Pt disk (0.078 cm²) was used as the working electrode. The cathodic and anodic potential sweeps (1 mV s⁻¹) were conducted on different cells. The electrolyte under investigation was soaked into a glass fiber separator (Whatmann GF/D). The platinum electrode was mechanically polished prior each measurement.

Li stripping-plating tests were conducted by means of cyclic voltammetry (1 mV s⁻¹ scan rate between -0.2 V and 0.2 V) using lithium for the counter and reference electrodes and a nickel disk (polished with diamond paste) as working electrode.

LiFePO_4 (Süd-Chemie-Clariant) and $\text{Li}_4\text{Ti}_5\text{O}_{12}$ (Sachtleben) were used as received. The electrodes were prepared following the procedure previously reported in Ref. [19]. In short, the active materials were mixed with conductive carbon (Cenergy, Super C65,

TIMCAL) and sodium-carboxymethylcellulose (CMC) binder (Walocel CRT 2000PA) by means of a planetary ballmill (Vario-Planetary Mill Pulverisette 4, FRITSCH) for more than 1 h. Prior coating the $\text{Li}_4\text{Ti}_5\text{O}_{12}$ slurry, 0.025 g of formic acid were added to reduce the pH and prevent the aluminum current collector corrosion. The resulting slurries were immediately casted on aluminum foils, using a laboratory blade coater. The coated tapes were dried at 80 °C for 1 h and then left at room temperature overnight. The final composition of the electrodes, expressed in weight ratio of the active material, conductive agent and binder, were 88:8:4 for LiFePO_4 and 87:8:5 for $\text{Li}_4\text{Ti}_5\text{O}_{12}$. Circular electrodes with a diameter of 12 mm were punched and dried at 180 °C under vacuum for 12 h. The electrode mass loading was about 3.5 mg cm⁻².

Galvanostatic tests were performed of half and full Li-ion cells. Lithium metal foil was used as counter and reference electrodes in half-cells. All the cells were left at OCV for 12 h before performing galvanostatic charge–discharge tests at different C-rates using a Maccor Battery Tester 4300. A C-rate of 1C corresponds to an applied current of 175 mA g⁻¹ and 170 mA g⁻¹ for $\text{Li}_4\text{Ti}_5\text{O}_{12}$ and LiFePO_4 respectively.

The full lithium ion cells, containing LiFePO_4 and $\text{Li}_4\text{Ti}_5\text{O}_{12}$ electrodes, were balanced using a cathode to anode weight ratio ranging from 1.1 to 1.2. Due to the practical delivered capacity, the resultant cells were all cathode limited. For comparison, full cells

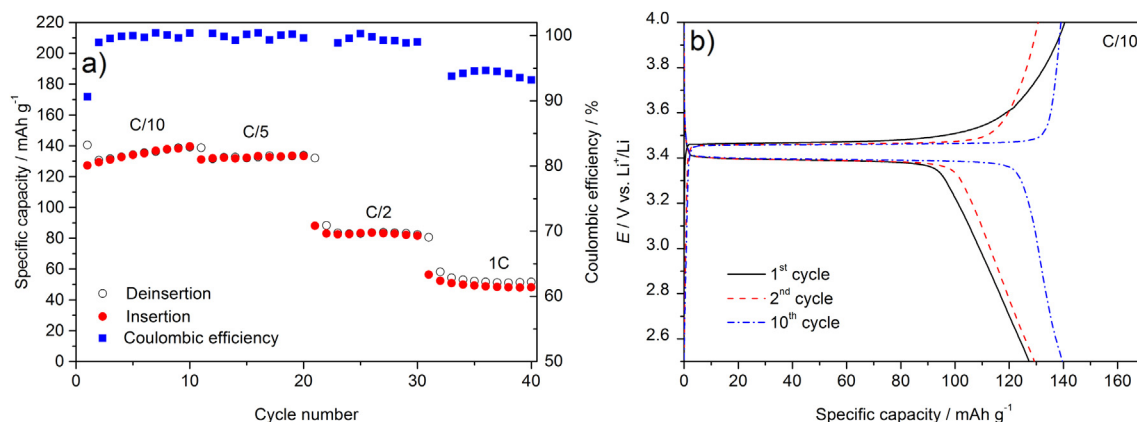


Fig. 5. a) Specific charge, discharge and coulombic efficiency obtained at different C-rates for LiFePO_4 electrodes in combination with $\text{PYR}_{1201}\text{FTFSI-LiFTFSI}$ (9:1) electrolyte. b) Voltage profiles for some selected cycles at C/10 rate.

with 1 M LiPF₆ in EC:DEC 3:7 conventional electrolyte were also assembled. All cells were cycled inside climatic chambers (Binder) to ensure constant temperature.

3. Results and discussions

3.1. Thermal measurement and conductivity

The DSC heating trace of PYR₁₂₀₁FTFSI-LiFTFSI 9:1 electrolyte is reported in Fig. 1. Only a glass transition at −98.1 °C (inflection point) is observed suggesting that the mixture remains amorphous down to −150 °C as in the case of the neat IL [12]. However, when the LiFTFSI salt is present, the glass transition occurs at slightly higher temperature with respect to pure PYR₁₂₀₁FTFSI (−104 °C) likely due to the interactions between lithium and FTFSI anions.

The phase behavior of the electrolyte was additionally investigated by measuring its ionic conductivity between −40 °C and 70 °C (with 2 °C steps) in order to reveal possible transitions that can be undetected by DSC [21]. The Arrhenius plot is reported in the inset of Fig. 1. During storage at −40 °C for 18 h, no changes in conductivity was detected. On increasing temperature the electrolyte conductivity increased showing values slightly lower than those reported for the neat IL. This is due to the increased viscosity of the IL-Li salt system as already demonstrated for other pyrrolidinium-based electrolytes [9]. At 20 °C the overall conductivity was $3.7 \times 10^{-3} \text{ S cm}^{-1}$, a value lower than that of mixtures of aliphatic carbonates but still adequate for low-power LIB applications.

3.2. Electrochemical tests

Fig. 2 shows the electrochemical stability window of the electrolyte under investigation. The potential value at which the current density flowing into the cell reached $\pm 0.1 \text{ mA cm}^{-2}$ is conventionally assumed as the anodic (E_a) stability limit. From Fig. 2 it is evident that the electrolyte is stable over a wide range of potential with the anodic limit approaching 5 V vs Li and the lithium plating occurs at −0.15 V vs Li. The small feature at about 1.5 V can reasonably be ascribed to low levels of water contamination (the associated current flow is 0.01 mA cm^{-1}) as already reported in the literature for the TFSI anion [22,23].

The reversibility of the lithium stripping-plating process was investigated by means of cyclic voltammetry using Ni as the working electrode. The results, reported in Fig. 3, show small peaks at ca. 1.25 V vs Li and 0.5 V vs Li, which can be attributed to the Li insertion into the native NiOx layer on the Ni electrode surface [24], preceding the bulk lithium deposition at about −0.05 V vs Li. The sharp peak at 0.035 V vs Li during the anodic scan corresponds to the reversible stripping of lithium. A rough calculation of the efficiency of the stripping-plating process, based on the estimation of the cathodic and anodic peaks area, gives a value approaching 70%, which is to be considered excellent by the comparison with other electrolytes. The feasibility of PYR₁₂₀₁FTFSI-LiFTFSI 9:1 as electrolyte in lithium batteries was tested, at room temperature, using either Li₄Ti₅O₁₂ or LiFePO₄ and lithium metal.

The results of the galvanostatic cycling test obtained for Li₄Ti₅O₁₂ electrodes are shown in Fig. 4. During the first intercalation at C/10 rate, the cell delivered about 170 mAh g^{-1} . In the following cycles the capacity slightly decreases to reach a stable value of 165 mAh g^{-1} . The voltage profiles, reported in panel b, reflect the typical two-phase process associated with the Li insertion/de-insertion into/from the titanate structure at around 1.55 V vs Li. However some irreversibility affects the first cycles as already reported in the case of aqueous processed Li₄Ti₅O₁₂ electrodes [19]. In the following cycles at C/5, the efficiency increases to more than 99% while a high discharge capacity is retained

(160 mAh g^{-1}). An attempt to further increase the cycling rates resulted in the drop of the electrochemical performance that can be attributed to the lower mobility of the Li ions in the IL with respect to conventional electrolytes.

The investigation of the electrode behavior in PYR₁₂₀₁FTFSI-LiFTFSI was extended to the LiFePO₄ cathode material. Fig. 5 (panel a) shows the specific charge/discharge capacity delivered by the LiFePO₄ at room temperature but different C-rates. The coulombic efficiency of the redox process is also reported. During the first cycle at C/10 the capacity values and the efficiency are quite low.

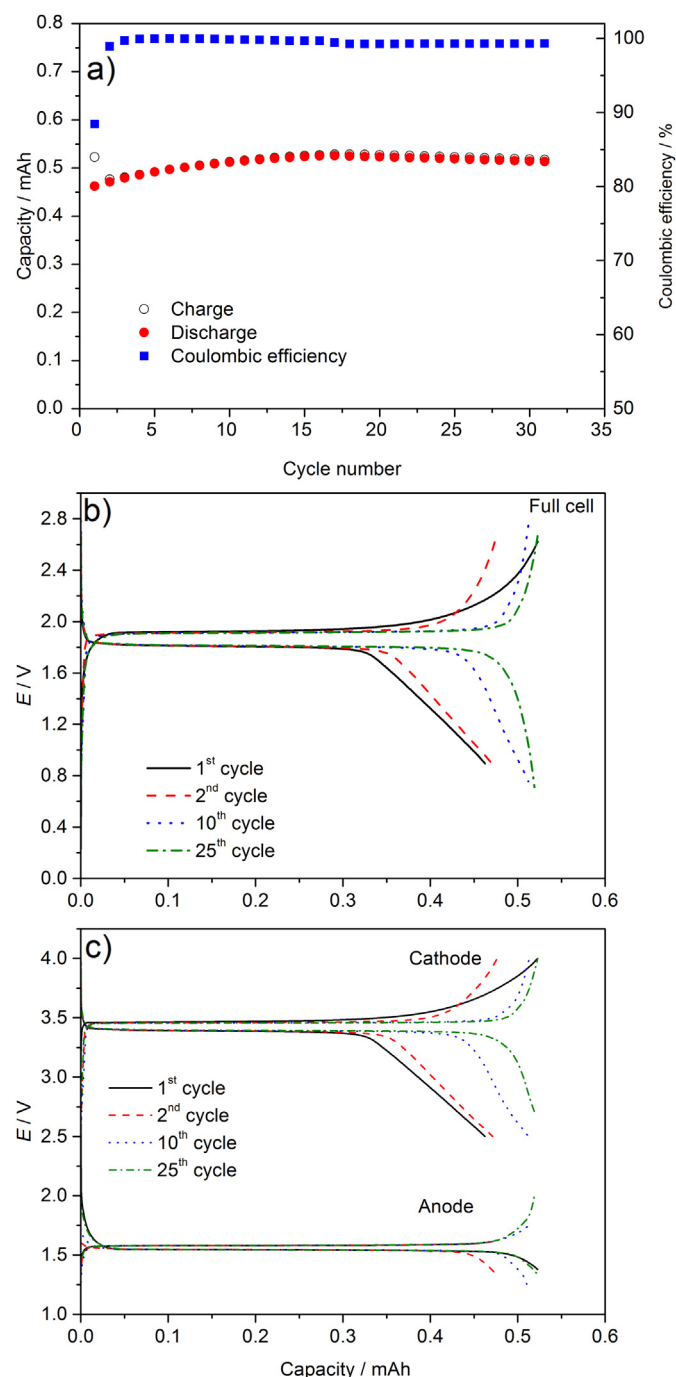


Fig. 6. a) Delivered capacity and coulombic efficiency vs. cycle number at C/10 charge/discharge rate for Li₄Ti₅O₁₂/LiFePO₄ cell with PYR₁₂₀₁FTFSI-LiFTFSI (9:1) electrolyte. b) Full-cell and c) separated anode and cathode voltage profiles for some selected cycles at C/10 rate.

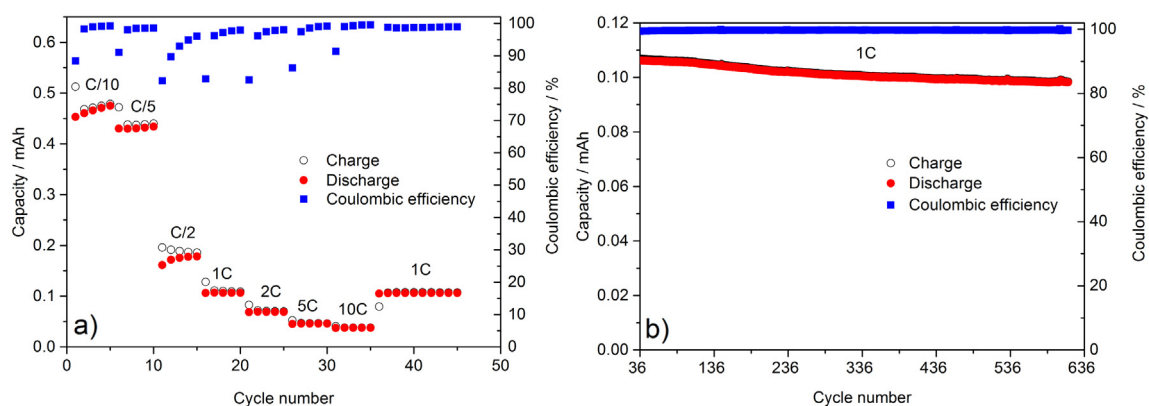


Fig. 7. a) Delivered capacity and coulombic efficiency vs. cycle number at different C-rates for $\text{Li}_4\text{Ti}_5\text{O}_{12}/\text{LiFePO}_4$ cell with $\text{PYR}_{1201}\text{FTFSI-LiFTFSI}$ (9:1) electrolyte. b) Long term cycling performance at 1C-rate. Note that this is the continuation of the C-rate test.

However, in the subsequent cycles the capacity increases reaching a value of about 140 mAh g^{-1} with a coulombic efficiency approaching 100%. Panel b of Fig. 5 reports the voltage profiles of some selected cycles at C/10 showing the characteristic plateau of LiFePO_4 at 3.4 V vs Li. During cycling, the plateau length increases while the cell polarization slightly decreases. The reason for such behavior can be ascribed to the higher viscosity of the IL-based electrolyte, which slows the wetting of the porous electrode. At a C/5 cycling rate, the cell delivers about 130 mAh g^{-1} while maintaining high efficiency values. A further increase of the cycling rate to C/2 resulted in a sudden drop of capacity to about 80 mAh g^{-1} . However, considering that the cells were cycled at room temperature, the obtained capacity values are among the highest obtained for LiFePO_4 in IL-based electrolytes [4,25–29].

Based on the promising results obtained from the half-cell tests, lithium ion cells with LiFePO_4 and $\text{Li}_4\text{Ti}_5\text{O}_{12}$ as active materials, and $\text{PYR}_{1201}\text{FTFSI-LiFTFSI}$ (9:1 mole ratio) electrolyte, were assembled. The results of galvanostatic cycling at room temperature are shown in Fig. 6. The cycling rate is calculated on the basis of the practical capacity of the cathode that limits the battery performance. As shown in panels a and b, the cell needed a few cycles before reaching a stable value of capacity of more than 0.500 mAh with a coulombic efficiency exceeding 99%, reflecting the behavior of the cathode described above. The cathode's influence becomes clear when inspecting the voltage profile of electrodes separately (Fig. 6c). During the first cycles the cathode reaches the cut-off voltage before the anode, but as the electrode wetting improves, the delivered capacity increases and thus the anode utilization. At the 25th cycle the discharge capacity was 0.519 mAh that corresponds to a specific capacity of 138 mAh g^{-1} and 160 mAh g^{-1} for

the cathode and the anode at 20°C , respectively. The energy density of the cell (calculated integrating the discharge curve of the 25th cycle) was 131 Wh kg^{-1} .

The results of the C-rate tests are reported in Fig. 7 (panel a). As seen during the half cell tests, the high rate performance is inferior to that obtainable with conventional electrolytes due to the higher viscosity and low conductivity of IL electrolytes at 20°C . However, it is worth noting that when the cycling rate is brought back to 1C, the cell completely recovers the previous capacity meaning that no electrode degradation occurred and the active materials are stable in contact with $\text{PYR}_{1201}\text{FTFSI-LiFTFSI}$ (9:1 mole ratio). The cell was then left to run at 1C as shown in Fig. 7b): the coulombic efficiency remained stable at values higher than 99% and after more than 500 cycles the capacity retention was higher than 90%.

The behavior of the full lithium-ion cell at high temperature was also investigated. The conventional carbonate-based electrolytes suffer of poor chemical stability at high temperatures leading to serious safety concerns. In comparison, the main key safety advantages of ILs are the low vapor pressure, non-flammability and high thermal stability. As a matter of fact, $\text{PYR}_{1201}\text{FTFSI}$ was shown to be stable up to 270°C in N_2 and up to 200°C in O_2 [12]. The cells were initially cycled at 20°C and C/10. Successively, the temperature was raised to 40°C , 60°C and 80°C with intermediate steps at 20°C . The cells were equilibrated for 3 h at each temperature before being subjected to cycling tests. During the intermediate steps at 20°C the cells were cycled at C/10 to evaluate the effect of the constant cycling at higher temperatures. For comparison purposes, an equivalent lithium ion cell with a carbonate based electrolyte (1 M LiPF_6 in EC:DEC 3:7) was also tested.

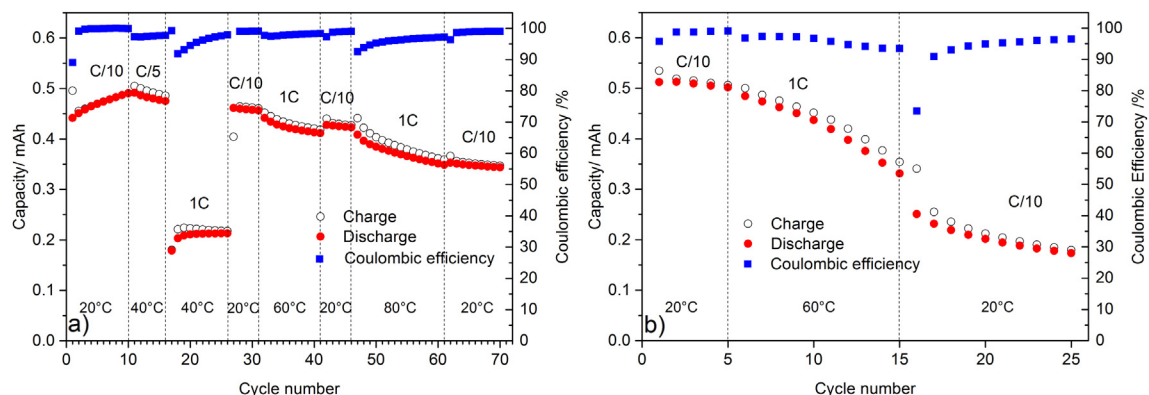


Fig. 8. Delivered capacity and coulombic efficiency vs. cycle number at different C-rates and temperatures for $\text{Li}_4\text{Ti}_5\text{O}_{12}/\text{LiFePO}_4$ cell with a) $\text{PYR}_{1201}\text{FTFSI-LiFTFSI}$ (9:1) electrolyte and b) 1 M LiPF_6 EC:DEC (3:7) electrolyte.

Panel a of Fig. 8 shows the charge/discharge capacity and the coulombic efficiency obtained for the cell with $\text{PYR}_{1201}\text{FTFSI-LiFTFSI}$ 9:1 electrolyte. After cycling at 40 °C the cell lost 6% of the initial capacity (as measured at C/10 and 20 °C). An additional 6% was lost after cycling at 60 °C, and after the last cycling at 80 °C the delivered capacity was 0.35 mAh that corresponds to 71.5% of the initial capacity. It is worth noting that even in the last cycles at 20 °C the coulombic efficiency reached 99%.

On the other hand, as shown in Fig. 8b), the lithium ion cell with carbonate-based electrolyte, after cycling at 60 °C showed a capacity retention of only 36% (measured at C/10 and 20 °C). In the last cycles at 20 °C the coulombic efficiency was only about 96%.

It is interesting to note that, at room temperature and low C rate, the performance of the cell containing $\text{PYR}_{1201}\text{FTFSI-LiFTFSI}$ (9:1) electrolyte is comparable to that of the cell made with conventional electrolyte. However the former displays good performance even at 60 °C and 1C rate.

4. Conclusions

The properties of $\text{PYR}_{1201}\text{FTFSI}$ doped with LiFTFSI have been studied to assess its possible use as an electrolyte for lithium-ion batteries. DSC and conductivity data showed that the electrolyte remains amorphous even at very low temperatures. The mixture is electrochemically stable in a wide potential range and lithium stripping-plating processes take place. Therefore this electrolyte is a good candidate to be used in combination with several electrode chemistries. In order to develop, not only safer, but also greener lithium ion batteries, all the electrodes used were manufactured avoiding the use of toxic solvents and fluorinated binders.

The electrochemical performance of $\text{Li}_4\text{Ti}_5\text{O}_{12}$ and LiFePO_4 in combination with $\text{PYR}_{1201}\text{LiFTFSI-LiFTFSI}$ 9:1 electrolyte was evaluated. Both electrode materials seem to be compatible with the new electrolyte system, delivering capacities close to the theoretical values at low cycling rates. However, the high rate cyclability is hampered by the IL viscosity. Full lithium ion cells based on a titanium anode and LiFePO_4 were assembled and tested. At 20 °C, the $\text{Li}_4\text{Ti}_5\text{O}_{12}/\text{PYR}_{1201}\text{LiFTFSI-LiFTFSI}/\text{LiFePO}_4$ cells showed a delivered stable capacity at low rate (C/10) of around 0.52 mAh that corresponds to an energy density of 131 Wh kg^{-1} , with a coulombic efficiency exceeding 99%.

Finally, the high temperature performance of lithium-ion cells using the IL-based electrolyte and a conventional organic electrolyte were compared. With this latter electrolyte, a loss of 64% of the initial cell capacity (as measured at 20 °C) was detected after cycling at 60 °C. Instead the IL-based cell was still able to deliver 71% of its initial capacity (at 20 °C) even after cycling at 80 °C.

In conclusion, we demonstrate that the electrolyte based on $\text{PYR}_{1201}\text{FTFSI}$ is suitable for applications in lithium-ion battery. We believe that the system is very promising as the results show that properly tailored ionic liquids can achieve the same performance as conventional electrolytes at low cycling rates, while at the same time guaranteeing improved safety, environmental compatibility and recyclability. Despite the fact that the viscosity hinders the high power application of the present electrolyte, its use permits a considerable extension of the temperature range of the battery while maintaining good performance. Due to the high conductivity

and wide electrochemical and thermal stability, this family of ionic liquids are also appealing for applications that require high energy density. Therefore electrochemical tests on different cell chemistries are in progress.

Acknowledgment

This work was supported by BMBF within the project “MEET Hi-END – Materialien und Komponenten für Batterien mit hoher Energiedichte” (Förderkennzeichen: 03X4634A).

The authors wish to thank Südchemie-Clariant, Sachtleben and Timcal for kindly providing the materials.

References

- [1] B. Scrosati, J. Garche, *J. Power Sources* 195 (2010) 2419–2430.
- [2] D. Aurbach, Y. Talyosef, B. Markovsky, E. Markevich, E. Zinigrad, L. Asraf, J.S. Gnanaraj, H.-J. Kim, *Electrochim. Acta* 50 (2004) 247–254.
- [3] K. Xu, *Chem. Rev.* 104 (2004) 4303–4418.
- [4] G.B. Appetecchi, M. Montanino, S. Passerini, Ionic liquid-based electrolytes for high energy, safer lithium batteries, in: *Ionic Liquids: Science and Applications*, American Chemical Society, 2012, pp. 67–128.
- [5] M. Armand, F. Endres, D.R. MacFarlane, H. Ohno, B. Scrosati, *Nat. Mater.* 8 (2009) 621–629.
- [6] A. Lewandowski, A. Świdarska-Mocek, *J. Power Sources* 194 (2009) 601–609.
- [7] M. Galiński, A. Lewandowski, I. Stepniak, *Electrochim. Acta* 51 (2006) 5567–5580.
- [8] G.B. Appetecchi, M. Montanino, M. Carewska, M. Moreno, F. Alessandrini, S. Passerini, *Electrochim. Acta* 56 (2011) 1300–1307.
- [9] Q. Zhou, P.D. Boyle, L. Malpezzi, A. Mele, J.-H. Shin, S. Passerini, W.A. Henderson, *Chem. Mater.* 23 (2011) 4331–4337.
- [10] E. Paillard, Q. Zhou, W.A. Henderson, G.B. Appetecchi, M. Montanino, S. Passerini, *J. Electrochem. Soc.* 156 (2009) A891–A895.
- [11] J. Reiter, E. Paillard, L. Grande, M. Winter, S. Passerini, *Electrochim. Acta* 91 (2013) 101–107.
- [12] J. Reiter, S. Jeremias, E. Paillard, M. Winter, S. Passerini, *Phys. Chem. Chem. Phys.* 15 (2013) 2565–2571.
- [13] G.A. Giffin, N. Laszczynski, S. Jeong, S. Jeremias, S. Passerini, *J. Phys. Chem. C* 117 (2013) 24206–24212.
- [14] Z.-B. Zhou, H. Matsumoto, K. Tatsumi, *Chem. Eur. J.* 12 (2006) 2196–2212.
- [15] H. Matsumoto, N. Terasawa, T. Umecky, S. Tsuzuki, H. Sakaebe, K. Asaka, K. Tatsumi, *Chem. Lett.* 37 (2008) 1020–1021.
- [16] J. Drofienik, M. Gaberscek, R. Dominko, F.W. Poulsen, M. Mogensen, S. Pejovnik, J. Jamnik, *Electrochim. Acta* 48 (2003) 883–889.
- [17] S.S. Jeong, N. Böckenfeld, A. Balducci, M. Winter, S. Passerini, *J. Power Sources* 199 (2012) 331–335.
- [18] A. Moretti, G.-T. Kim, D. Bresser, K. Renger, E. Paillard, R. Marassi, M. Winter, S. Passerini, *J. Power Sources* 221 (2013) 419–426.
- [19] G.T. Kim, S.S. Jeong, M. Joost, E. Rocca, M. Winter, S. Passerini, A. Balducci, *J. Power Sources* 196 (2011) 2187–2194.
- [20] G.B. Appetecchi, S. Scaccia, C. Tizzani, F. Alessandrini, S. Passerini, *J. Electrochem. Soc.* 153 (2006) A1685–A1691.
- [21] A. Triolo, O. Russina, B. Fazio, G.B. Appetecchi, M. Carewska, S. Passerini, *J. Chem. Phys.* 130 (2009).
- [22] S. Randström, M. Montanino, G.B. Appetecchi, C. Lagergren, A. Moreno, S. Passerini, *Electrochim. Acta* 53 (2008) 6397–6401.
- [23] S. Randström, G.B. Appetecchi, C. Lagergren, A. Moreno, S. Passerini, *Electrochim. Acta* 53 (2007) 1837–1842.
- [24] G.T. Kim, G.B. Appetecchi, M. Carewska, M. Joost, A. Balducci, M. Winter, S. Passerini, *J. Power Sources* 195 (2010) 6130–6137.
- [25] P. Reale, A. Fericola, B. Scrosati, *J. Power Sources* 194 (2009) 182–189.
- [26] A. Fericola, F. Croce, B. Scrosati, T. Watanabe, H. Ohno, *J. Power Sources* 174 (2007) 342–348.
- [27] I. Quinzen, S. Ferrari, E. Quartarone, C. Tomasi, M. Fagnoni, P. Mustarelli, *J. Power Sources* 237 (2013) 204–209.
- [28] N. Wongtharom, T.-C. Lee, C.-H. Hsu, G. Ting-Kuo Fey, K.-P. Huang, J.-K. Chang, *J. Power Sources* 240 (2013) 676–682.
- [29] J. Jin, H.H. Li, J.P. Wei, X.K. Bian, Z. Zhou, J. Yan, *Electrochem. Commun.* 11 (2009) 1500–1503.